Supporting Information

The Intrinsic Volumetric Capacitance of Conducting Polymers: Pseudo-Capacitors or Double-Layer Supercapacitors?

*Ihor Sahalianov, Sandeep Kumar Singh, Klas Tybrandt, Magnus Berggren, and Igor Zozoulenko**

S1. Capacitance of crystallites

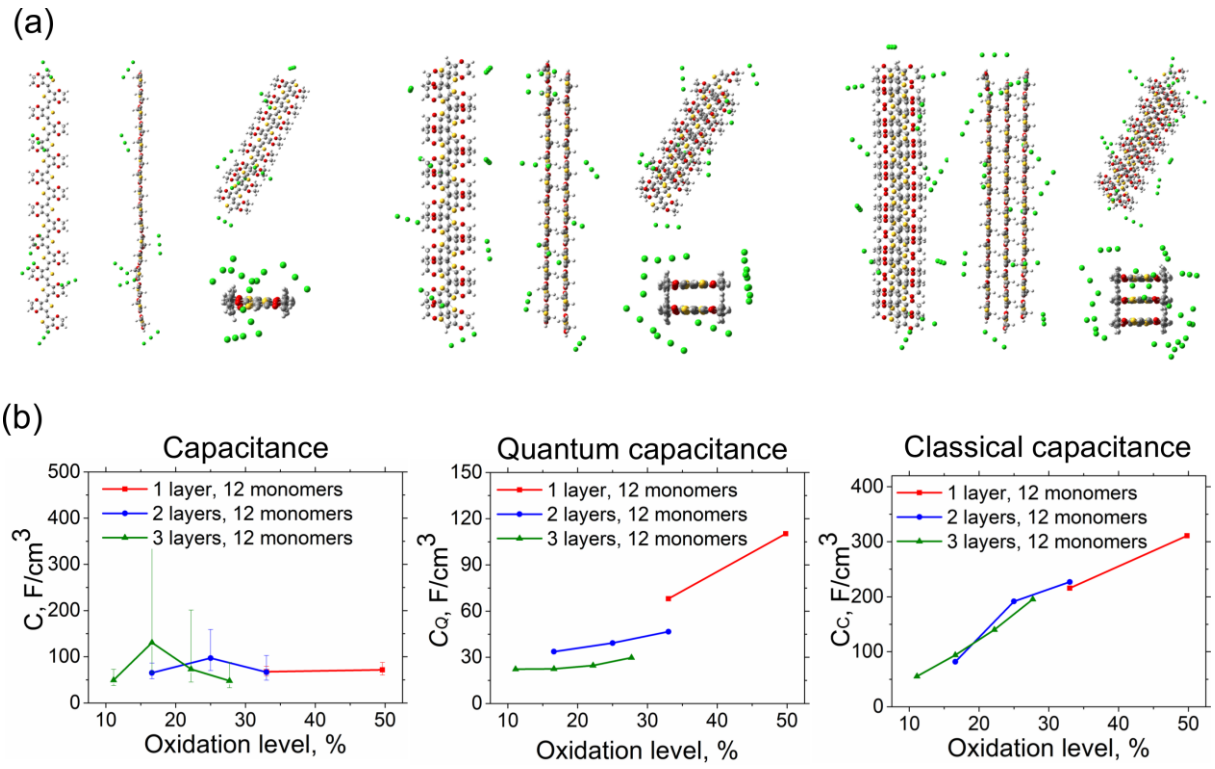

Figure S1: (a) Representative PEDOT crystallites composed of one, two and three PEDOT chains surrounded by counterions. (c) The total, quantum and classical capacitance of PEDOT crystallites. Carbon atoms are shown in grey, oxygens in red, sulphur in yellow, and chlor counterions in green.

S2. Representative distribution of counterions

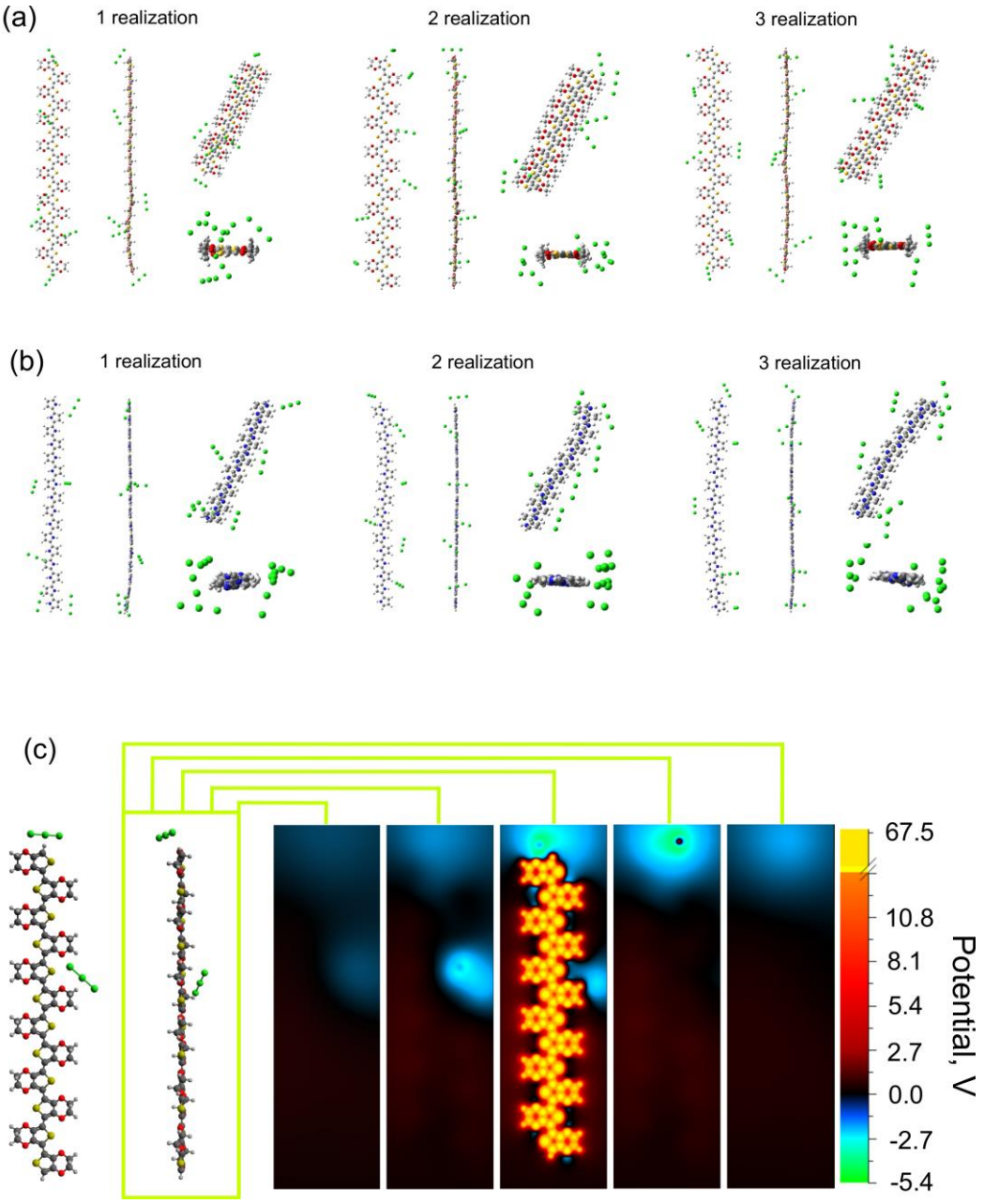

Figure S2: Representative distributions of counterions surrounding (a) PEDOT and (b) PPy chains for three different realizations. Carbon atoms are shown in grey, oxygens in red, sulphur in yellow, nitrogen in blue, and chlor counterions in green. (c) Potential distribution for a representative counterion configuration for *N*=12 PEDOT oligomer. Different images correspond to different planes at different distances from the PEDOT oligomers as shown in the figure.

S3. Dependence of the classical capacitance C_C on the cutoff radius R_{cutoff} and the size of the computational domain.

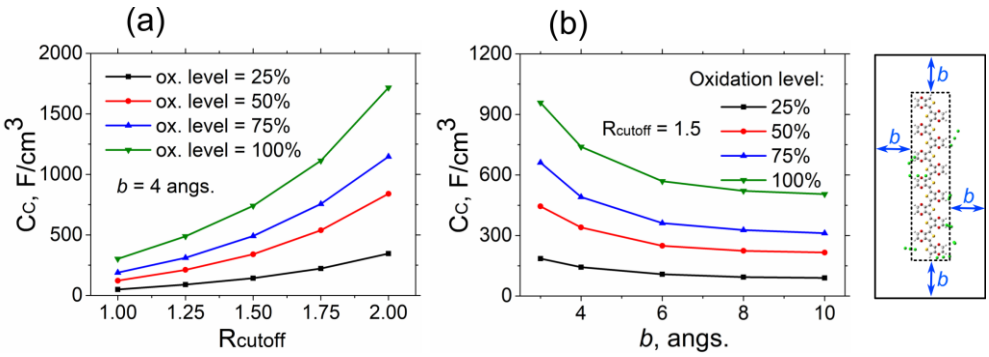

Figure S3: Dependence of C_C on (a) the cutoff radius R_{cutoff} and (b) the size of the computational domain. Calculations correspond to the PEDOT chain of the length N=12. R_{cutoff} is given in units of the van der Waals radius of the atoms composing the PEDOT chain.

S4. Comparison of 6-31g(d) and 6-31g(d)+ basis sets

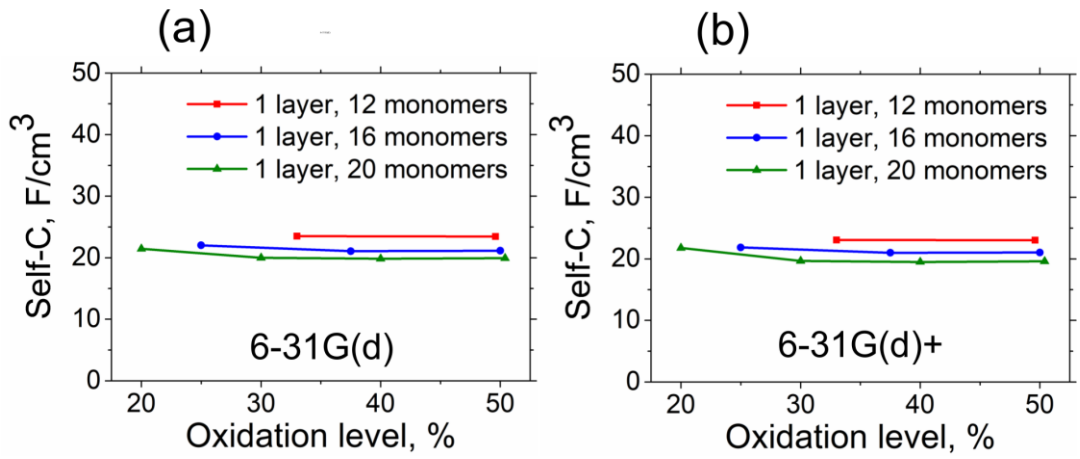

Figure S4: The self-capacitance calculated for basis sets (a) 6-31g(d) and (b) 6-31g(d)+. Simulations were carried out for three single-layer PEDOT samples with 12, 16 and 20 monomers with the fully optimized geometries. The difference between obtained results is negligible, hence, all results reported in this study are performed with the 6-31g(d) basis set without the diffusive functions to boost a computational speed.

S5. Averaging over different disorder realizations.

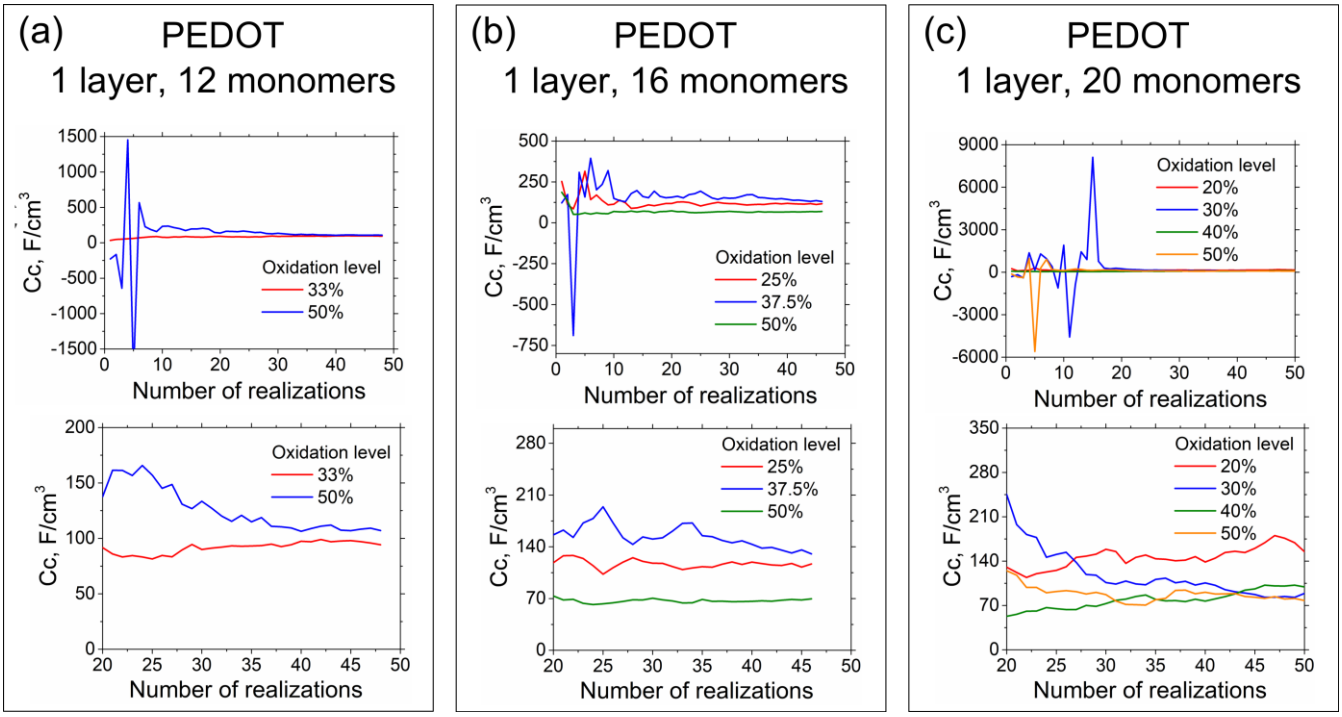

Figure S5. The dependence of the capacitance on the number of different counterion realizations for a PEDOT chains with a different number of counterions N. (a) N=12, (b) N=16, (c) N=20. Lower panels show zoomed images of the upper plots in the interval $20 \leq n_{realizations} \leq 50$.

S6. Definition of the volumetric capacitance

In order to calculate the volumetric capacitance we divide the calculated capacitance of each polymer sample by its overage volume $V = N\,V_{mon}$ where N is a number of monomers in a considered oligomer (N=12,16,20), and V_{mon} is a volume per one monomer which is calculated as described below.

The following mass densities of PEDOT and PPy are used, ρ_{PEDOT}=1.49 g/cm^3 (Ref. [1]) and ρ_{PPy}=2.1 g/cm^3 (Ref. [2]).

Consider, for example the case of N=12 oligomer. Calculation of the mass of one PEDOT chain gives,

$$M_{mol}^{PEDOT} = 2\mathrm{H} + [\mathrm{C_2H_4O_2C_4S}]_{12}$$

$$M_{mol}^{PEDOT} = 2 * 1.008 + 12(6 * 12.011 + 4 * 1.008 + 2 * 15.999 + 32.065)$$

$$= 1683.95\ g/mol$$

$$m_{PEDOT} = \frac{M_{mol}^{PEDOT}}{N_A} = \frac{1683.95}{6.02 * 10^{23}} = 2.8 * 10^{-21} g$$

Calculation of the mass of one PPy chain gives,

$$M_{mol}^{PPy} = 2\mathrm{H} + [\mathrm{C_2H_2C_2NH}]_{12}$$

$$M_{mol}^{PPy} = 2 * 1.008 + 12(4 * 12.011 + 3 * 1.008 + 14.007) = 782.92\ g/mol$$

$$m_{PPy} = \frac{M_{mol}^{PPy}}{N_A} = \frac{782.92}{6.02 * 10^{23}} = 1.3 * 10^{-21} g$$

Finally, volumes per monomer and per oligomer are as follows,

PEDOT:

$$V_{PEDOT} = \frac{m_{PEDOT}}{\rho_{PEDOT}} = \frac{2.8 * 10^{-21} g}{1.49\ g/cm^3} = 1.9 * 10^{-21} cm^3$$

$$V_{PEDOT}^{mon} = \frac{V_{PEDOT}}{12} = \frac{1.9 * 10^{-21} cm^3}{12} = 1.58 * 10^{-22} cm^3$$

PPy:

$$V_{PPy} = \frac{m_{PPy}}{\rho_{PPy}} = \frac{1.3 * 10^{-21} g}{2.1\ g/cm^3} = 0.62 * 10^{-21} cm^3$$

$$V_{PPy}^{mon} = \frac{V_{PPy}}{12} = \frac{0.62 * 10^{-21} cm^3}{12} = 0.52 * 10^{-22} cm^3$$

Thanks to the higher density and lower molecular weight, effective volume per monomer in PPy:TOS is three times smaller than the volume per monomer in PEDOT:TOS. Note that for simplicity in the above calculations the changes in the mass density due to the change of the oxidation level were omitted.

S7. Computational boxes used for calculations of the classical capacitance.

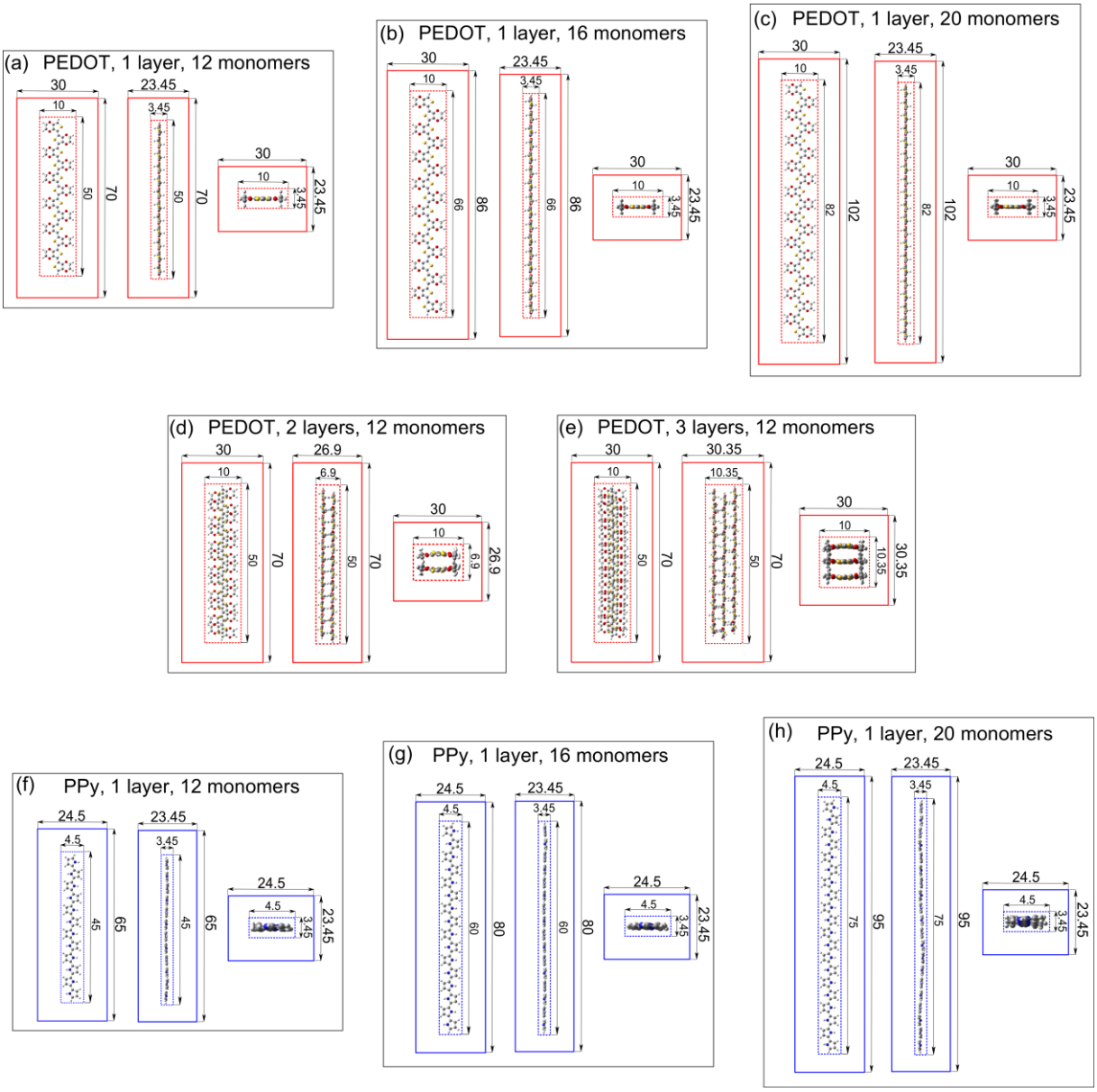

Figure S7. Parameters of simulation boxes for single-layer PEDOT (a,b,c), multilayer PEDOT (d,e) and single-layer PPy (f,g,h). All sizes are given in Å. Boundaries of polymers are depicted by dotted lines, boundaries of simulation boxes are shown with solid lines.

S8. Capacitance calculations with a pre-optimized geometry of polymers chains

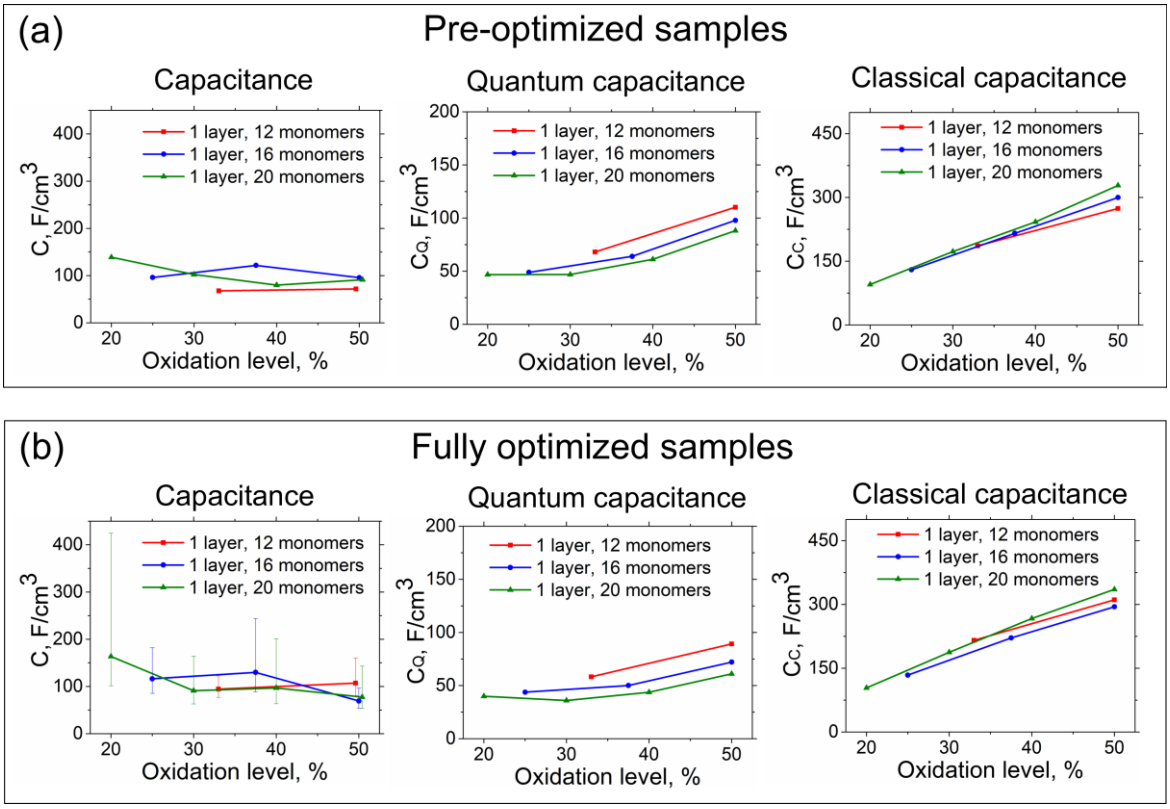

Figure S8. Comparison of the capacitance for the cases of pre-optimized the fully optimized geometries for PEDOT chains (upper and lower panels respectively). (a) Total capacitance, (b) quantum capacitance, (c) classical capacitance. PEDOT chains consist of 12, 16 or 20 monomers as indicated in the figure. Note that the lower panel in the figure is the same as the upper panel in Figure 2 in the main text and is displayed here for a convenience of the comparison.

Using pre-optimized samples is an efficient way to speed up the capacitance calculations with a minor decrease of accuracy. The calculations are performed in the following way. For instance, we want to calculate averaged total energy for the sample with N_{ions} counterions for N_{realiz} different spatial realizations. Instead of performing geometrical optimizations for all N_{realiz} realizations, we optimize only one sample without counterions with the total charge Q =

+ N_{ions}. Then, we use this pre-optimized geometry to perform a single-point energy calculation for each of these N_{realiz} different counterions locations. As a result, the calculations are typically 10-15 times faster. Note however that calculations for non-optimized geometries become more unstable. This approach allows us to calculate the capacitance of much bigger systems including crystallites containing several chains when a full geometrical optimization becomes too computationally expensive. Figure S8 shows the capacitance of PEDOT chains of different lengths N=12, 16 or 20 monomers calculated with and without full optimization. The obtained values of the capacitance are in a good quantitative agreement with each other.

S9. Hartree-Fock capacitance calculations.

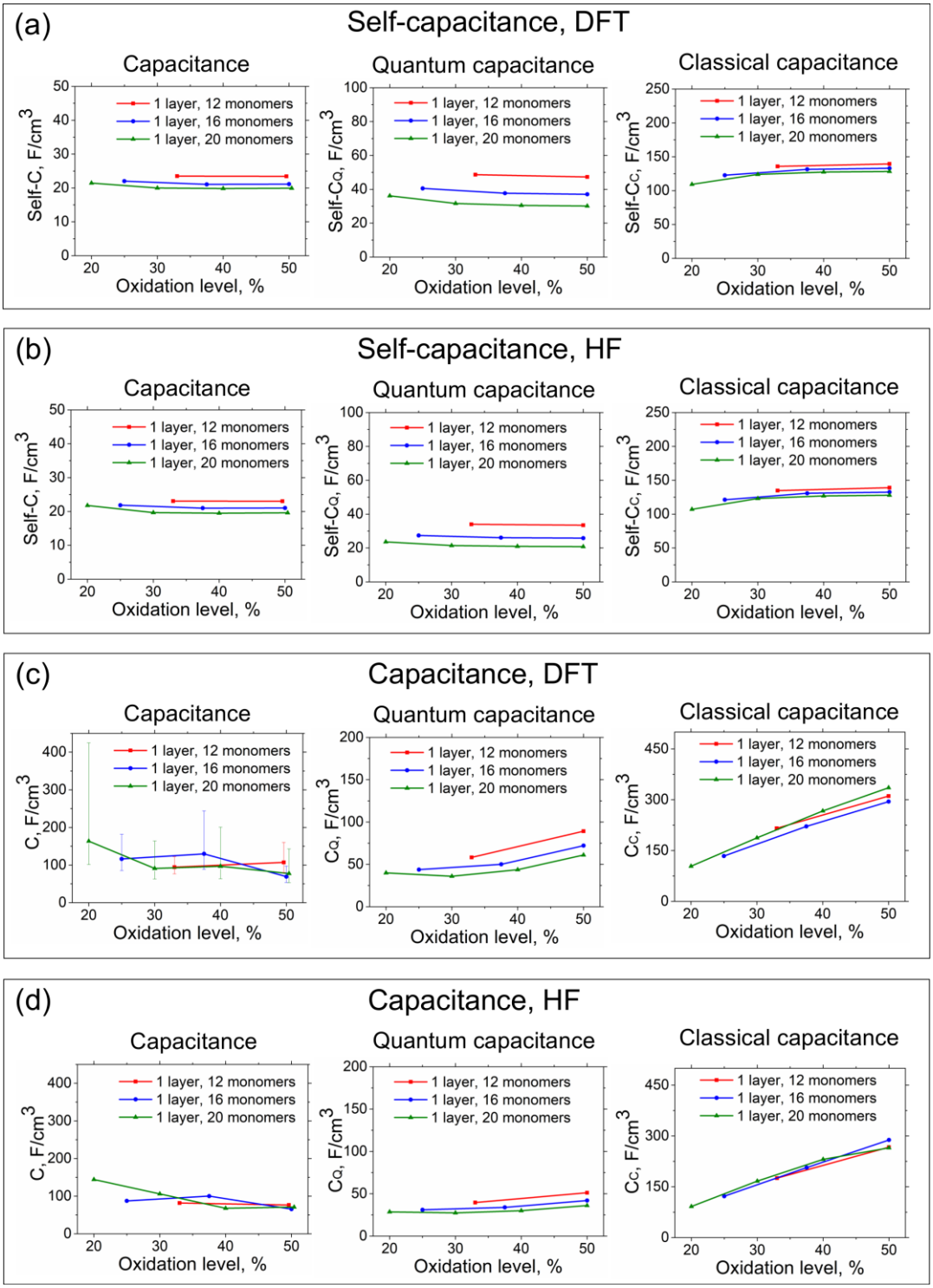

Figure S9: Comparison of the calculated (a),(b) self-capacitance and (c),(d) capacitance using the DFT and Hartree-Fock approaches. The total capacitances, quantum, and classical capacitances are calculated for PEDOT oligomers of the lengths N=12,16,20 as indicated in

figures. Data in (a), (b) and (c) were calculated for fully optimized structures. Capacitances of oligomers with counterions, obtained with HF method (d) were calculated for the pre-optimized structures.

While DFT calculations were performed for fully optimized systems, HF calculations were carried out for the DFT pre-optimized systems as those described in Sec. S8. That is, that polymers without counterions are initially optimized using DFT calculations and the final single point calculations of the electronic structure and natural population analysis charges are performed with the restricted HF in Gaussian16.

Table S1. Comparison between HF and DFT calculations. Total capacitances were obtained after averaging among the capacitances for all considered oxidation levels of all considered chains. Quantum capacitances were calculated after averaging among capacitances for oxidation levels < 40% (C_Q rapidly grows with a further increase of the oxidation level). Classical capacitance is calculated for the oxidation level 33% (corresponding to a pristine (as oxidized) PEDOT:PSS blend)

Method	Self C, F/cm^3	C, F/cm^3	Self C_Q, F/cm^3	C_Q, F/cm^3	Self C_C, ox=33%, F/cm^3	C_C, ox=33%, F/cm^3
DFT	21.4	105	37.5	45.3	135.8	215.7
HF	21.2	85.8	25.6	31.7	134.8	175.5

A comparison between the DFT and HF calculated results is summarized in Table S1. The total capacitances and the quantum capacitancies calculated based on the HF approach are ~ 20–30%

smaller than corresponding DFT results. Classical capacitance is almost unaffected by choosing of the calculation method. This is because of the similarity between electrostatic potential obtained within the DFT and HF methods. The good agreement between the DFT and HF results demonstrates that HF method can potentially be used in the calculation of the capacitance in the cases when DFT fails to achieve converged results, for instance, in systems with extremely high oxidation level or large distance between charged molecules (>4 Å).

S10. Numerical calculations of the classical capacitance.

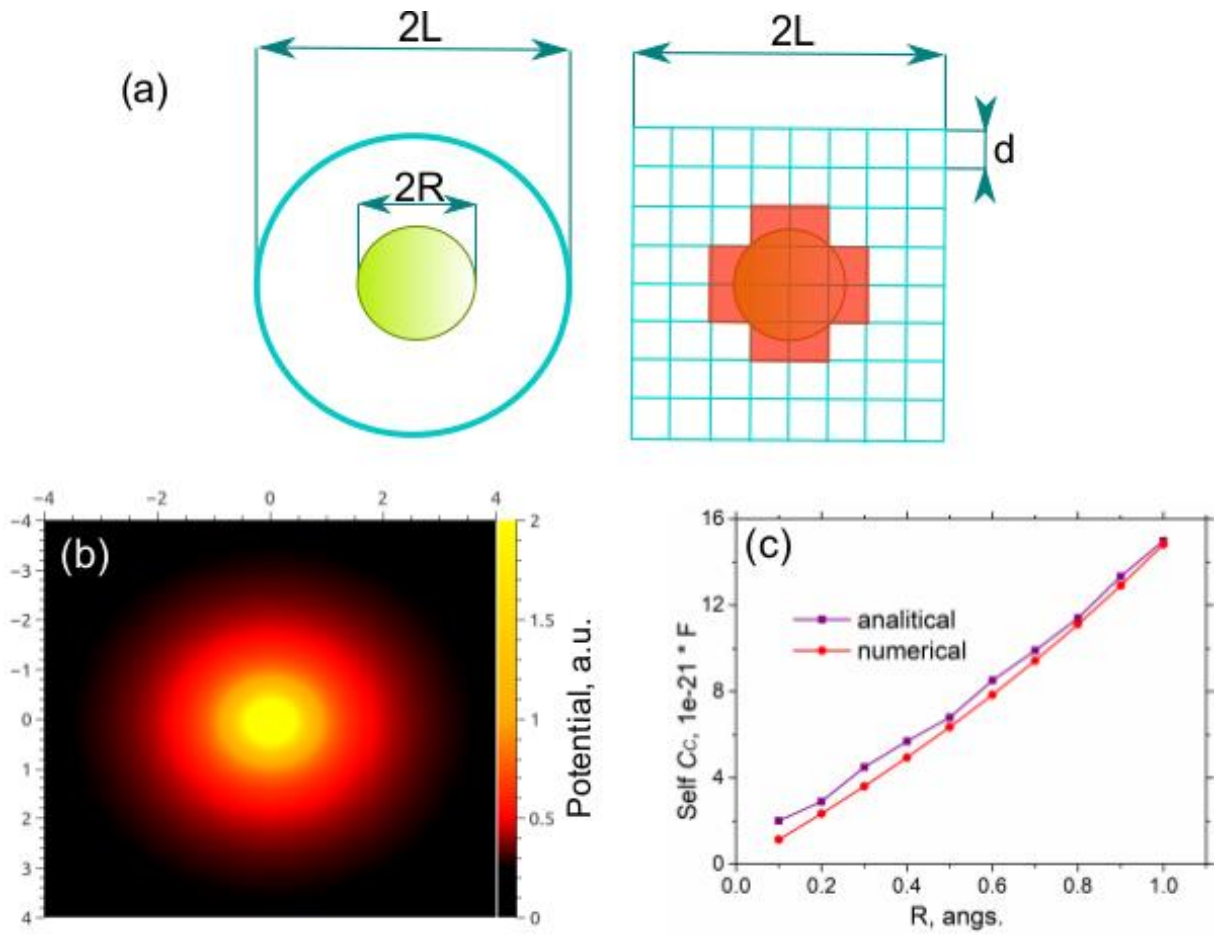

Figure S10: Calculations of a classical self-capacitance for a charged sphere. (a) A visualization of the charged sphere for analytical and numerical calculations of the self-capacitance. (b) The calculated electrostatic potential surface for the charged sphere in a computational box. (c) A comparison between the analytical results and numerical calculations.

To evaluate the accuracy of the numerical calculations of classical capacitance on a rectangular grid we calculate the self-capacitance of a charged metallic sphere and compare it with the analytical results. The self-capacitance of a sphere of a radius R is given by the expression, $C = 4\pi\varepsilon_0 R$. This is an exact expression for the sphere in infinite space. If,

instead, the integration of the electric field is limited to a spherical region of the radius L as illustrated in Figure S5, the corresponding analytical expression reads,

$$C = 4\pi\varepsilon_0 \frac{L*R}{L-R}. \quad \text{(S1)}$$

In numerical calculation a charged metallic sphere is placed in the center of a cubic simulation box $L\times L\times L$ as illustrated in Figure S5a, with the size L=4 Å, and a uniform cubic 3D grid with the step d = 0.2 Å in each direction.

Numerical simulations were performed in several steps:

1) Potential of the metallic sphere was extracted using Mulfiwfn software package[3], designed to supplement Gaussian16 calculations. Electric field was calculated from the potential according to $\vec{E} = -\nabla V$. (Note that in Gaussian calculation the metallic sphere was represented by a point charge where the electric field at each grid point inside the sphere was set to zero as illustrated in Figure S10a in order to account for the metallic character of the sphere.)

2) Numerical integration of the $|E|^2$ in the simulation box was performed on the square grid and the classical capacitance is calculated according to Equation 11.

Figure S10c shows a comparison between the numerical calculations and analytical expression given by Equation S1, where the self-capacitance is calculated for different sizes of the sphere. A good agreement between the numerical calculations and analytical results provides a justification for the chosen numerical method and the grid size of the computational box.

1. K. E. Aasmundtveit, E. J. Samuelsen, L. A. A. Pettersson, O. Inganäs, T. Johansson, R. Feidenhans, *Synthetic Metals*, 1999, **101**, 561.

2. P. Holzhauser K. Bouzek, *Journal of applied electrochemistry*, 2006, **36(6)**, 703.

3. T. Lu, F. Chen, *Journal of computational chemistry*, 2012, **33(5)**, 580.